

# Linking the Development of Ventilator-Induced Injury to Mechanical Function in the Lung

BRADFORD J. SMITH, KARA A. GRANT, and JASON H. T. BATES

Vermont Lung Center, University of Vermont College of Medicine, 149 Beaumont Avenue, HSRF 228, Burlington, VT 05405-0075, USA

(Received 16 September 2012; accepted 1 November 2012; published online 16 November 2012)

Associate Editor John H. Linehan oversaw the review of this article.

**Abstract**—Management of ALI/ARDS involves supportive ventilation at low tidal volumes ( $V_t$ ) to minimize the rate at which ventilator induced lung injury (VILI) develops while the lungs heal. However, we currently have few details to guide the minimization of VILI in the ALI/ARDS patient. The goal of the present study was to determine how VILI progresses with time as a function of the manner in which the lung is ventilated in mice. We found that the progression of VILI caused by over-ventilating the lung at a positive end-expiratory pressure of zero is accompanied by progressive increases in lung stiffness as well as the rate at which the lung derecruits over time. We were able to accurately recapitulate these findings in a computational model that attributes changes in the dynamics of recruitment and derecruitment to two populations of lung units. One population closes over a time scale of minutes following a recruitment maneuver and the second closes in a matter of seconds or less, with the relative sizes of the two populations changing as VILI develops. This computational model serves as a basis from which to link the progression of VILI to changes in lung mechanical function.

**Keywords**—Mouse model, Lung elastance, Alveolar flooding, Surfactant dysfunction, Computational model.

## INTRODUCTION

The key to clinical management of patients with acute respiratory distress syndrome (ARDS) is avoidance of additional ventilator-induced lung injury (VILI). In general terms, this amounts to ventilating with a small tidal volume ( $V_t$ ) to avoid volutrauma, and applying positive end-expiratory pressure (PEEP) to avoid atelectrauma.<sup>23,24</sup> Current clinical practice

adopts a one-size-fits-all strategy based on these principles, as exemplified by the ARDSNet recommended  $V_t$  of 6 mL/kg ideal body weight,<sup>1</sup> yet ARDS patients are not all the same. Indeed, it seems axiomatic that improvements in management will be achieved if personalized ventilatory strategies can be developed that take a particular patient's injury status into consideration. Such strategies will have to be based on clinical parameters that can be measured rapidly and continually, and that reflect the development of VILI.

The obvious candidates to act as guides for the minimization of VILI are parameters that reflect lung mechanical function because they can be measured noninvasively from pressure-flow relationships assessed at the tracheal opening,<sup>6</sup> and because VILI is an inherently mechanical process. For such parameters to be useful in this regard, however, we would have to know how the mechanical properties of the lung reflect the risk of causing VILI in any given individual, something that we currently understand little about. Accordingly, the goal of the present study was to determine how the development of VILI is reflected in measurable changes in lung mechanics.

We undertook our study in mice because we have previously shown that VILI can be made to develop in a progressive and accelerating manner in this species when they are ventilated for several hours with a large  $V_t$  at a PEEP of zero.<sup>34</sup> This allowed us to titrate the acceleration of lung injury through adjustment of  $V_t$  in order to determine quantitative relationships between the rate at which VILI develops and certain key parameters of lung mechanics. We then attempted to recapitulate these findings in a computational model as an aid to understanding how the biophysical effects of fluid and protein accumulation in the pulmonary airspaces might manifest at the organ level.

---

Address correspondence to Jason H. T. Bates, Vermont Lung Center, University of Vermont College of Medicine, 149 Beaumont Avenue, HSRF 228, Burlington, VT 05405-0075, USA. Electronic mail: jason.h.bates@uvm.edu

## MATERIALS AND METHODS

### *Animal Procedures*

Experiments were conducted on healthy 8–10 week old BALB/c mice (Jackson Laboratories, Bar Harbor, ME) weighting 18.3–24.2 g (average 21.9 g). The mice were anesthetized with 90 mg·kg<sup>-1</sup> intraperitoneal (IP) sodium pentobarbital, and a modified 18 gauge PrecisionGlide needle (Becton Dickson & Co., NJ) was surgically inserted into the trachea. The cannula was then attached to a programmable computer-controlled small animal ventilator (flexiVent, SCIREQ, Montreal, QC, Canada) and baseline ventilation was started with a tidal volume ( $V_t$ ) of 0.25 mL at a frequency of 200 breaths·min<sup>-1</sup> against a PEEP of 3 cmH<sub>2</sub>O. Because of gas compressibility within the ventilator cylinder, the  $V_t$  delivered to the lung was 0.2 mL, or 2 L kg<sup>-1</sup> min<sup>-1</sup>. Baseline ventilation was applied for an initial 20 min stabilization period, after which a 4 h experimental protocol was applied (see below). The mice were given an IP injection of 0.5 mL kg<sup>-1</sup> pancuronium bromide at the beginning of the stabilization period to prevent any spontaneous breathing efforts. Subsequent IP injections of 5 mg kg<sup>-1</sup> sodium pentobarbital were administered approximately every 30 min to maintain deep anesthesia. To ensure adequate anesthesia under paralysis, heart rate was monitored continuously *via* electrocardiogram. At the conclusion of the experimental protocol the animals were euthanized with an IP injection of 150 mg kg<sup>-1</sup> pentobarbital followed by cervical dislocation. This protocol was approved by the Institutional Animal Care and Use Committee of the University of Vermont, and animal treatment was in compliance with the Animal Welfare Act.

### *Experimental Protocol*

Following the 20 min baseline ventilation period, a deep inhalation (DI) was administered by briefly inflating the lung to 30 cmH<sub>2</sub>O in order to recruit any lung regions that might have previously become closed. PEEP was then set to 0, a second DI was applied, and respiratory system impedance was determined using a 2 s multi-frequency (0.5–20.5 Hz) displacement of the ventilator cylinder (amplitude 0.17 mL). The impedance was fit with the constant-phase model<sup>16</sup> from which a measure of lung elastance ( $H$ ) was obtained, as we have described in previous studies.<sup>3–5,33,34</sup>

The animals were then subjected to a 4 h ventilation protocol that began with a test of derecruitability. This test consisted of ventilating the animals with a  $V_t$  of 0.25 mL for 4.5 min during which  $H$  was determined every 20 s. We have established previously<sup>4</sup> that the rise

in  $H$  over this brief period reflects the propensity of the lungs to derecruit over time. Immediately following the derecruitability test, the mice were ventilated for 16.5 min with a large  $V_t$ . Four over-ventilation volumes of 1.0, 1.1, 1.2, and 1.3 mL were investigated in separate groups of mice at a frequency of 50 breaths min<sup>-1</sup>, corresponding to means of 45.7, 51.0, 52.3, and 60.0 mL kg<sup>-1</sup>, respectively. During this over-ventilation epoch, peak tracheal pressures ( $\overline{P_{tr}}$ ) were recorded at 5.5 min intervals. This sequence of derecruitability test followed by over-ventilation was applied repeatedly until either the total time elapsed was 4 h or the animal died.

### *Computational Modeling*

We simulated the dynamics of lung recruitment and derecruitment using an adaptation of a computational model that we have previously described in detail.<sup>7,22</sup> The model consists of  $N = 1200$  parallel lung units, a number selected arbitrarily to provide a balance between computational efficiency and smoothness of the simulations. The lung units are identical, each with an elastance,  $E_{unit}$ , that increases linearly with unit volume,  $V_{unit}$ , in order to mimic the strain stiffening observed in the lung.<sup>32</sup> We also allow the stiffness of each unit to increase linearly with time as a result of progressive VILI. The equation governing the overall behavior of  $E_{unit}$  is

$$E_{unit}(t, V_{unit}) = N[E_{base} + (1 + E_{damage}t) * (V_{unit}NE_{strain})] \quad (1)$$

where  $E_{base} = 20$  cmH<sub>2</sub>O mL<sup>-1</sup> is the zero-volume elastance in the healthy lung,  $E_{strain} = 14$  cmH<sub>2</sub>O mL<sup>-2</sup> is a constant that accounts for strain stiffening of the lung tissue, and  $E_{damage} = 6 \times 10^{-6}$  accounts for damage-induced stiffening.

The units of the model are either open (recruited) or closed (derecruited). The elastance of the entire lung model,  $H_{mod}$ , is thus a function of the number,  $N_{open}(t)$ , of open units thus:

$$H_{mod}(t) = 1 / \sum_{\text{Open units}} \frac{1}{E_{unit}(t, V_{unit})}. \quad (2)$$

Each lung unit is connected to a common junction by an airway of fixed resistance  $R_{unit}$ , where

$$R_{unit} = NR_{aw} \quad (3)$$

and  $R_{aw}$  is total airway resistance set equal to 0.47 cmH<sub>2</sub>O s mL<sup>-1</sup> to match baseline measurements made in the mice. The overall resistance of the lung at any point in time is then

$$R_L(t) = \frac{R_{unit}(t)}{N_{open}(t)}. \quad (4)$$

Dynamic closure and reopening of the parallel airways in the model is simulated using virtual trajectories as we have previously described.<sup>7,21,22</sup> Briefly, each airway is either fully open or fully closed, and is associated with a virtual trajectory specified by a variable,  $x$ , that may take a value on the open interval  $(0, 1)$ . The value of  $x$  increases if the pressure,  $P$ , that is applied to the airway is greater than a specified critical opening pressure,  $P_o$ , with the rate of increase being  $s_o(P - P_o)$  where  $s_o$  is an opening velocity constant. The converse occurs if  $P$  is less than a critical closing pressure,  $P_c$ , with the rate of decrease in  $x$  being  $s_c(P_c - P)$  where  $s_c$  is a closing velocity constant. If the airway is open and  $x$  reaches 0 then the airway immediately closes, and conversely if the airway is closed and  $x$  reaches 1 it opens immediately. The recruitment and derecruitment behavior of the entire model is thus determined by the distributions from which the values of  $P_o$ ,  $P_c$ ,  $s_o$  and  $s_c$  are randomly drawn (see “Results” section).

The model was driven during inspiration through the airway junction by a specified volume waveform buffered by the elastance,  $E_{\text{gas}}$ , of an intervening volume of gas representing that in the cylinder and connecting tubing of the ventilator.  $E_{\text{gas}}$  was set equal to  $130 \text{ cmH}_2\text{O mL}^{-1}$  to match the value determined for the experimental ventilator. The inspiratory volume waveform was a half-sinusoid of appropriate frequency and amplitude. Expiration from the model was passive, being driven by the elastic recoil pressures in the open units that emptied through their respective airways and then through a conduit representing the tubing of the equipment with resistance  $R_{\text{eq}} = 0.4 \text{ cmH}_2\text{O s mL}^{-1}$ .

The model equations were specified and integrated numerically with a time step of  $0.005 \text{ s}$  as described previously by Massa *et al.*<sup>22</sup> Fitting was accomplished with a GNU Scientific Library implementation of the Simplex algorithm described by Nelder and Mead,<sup>26</sup> a derivative-free approach to minimizing the fit error between the predicted and measured data. However, because of the presence of local minima, manual adjustment of the parameters was necessary and the simplex algorithm served to refine these estimates. This model fitting procedure was computational expensive, requiring multiple runs of the model using different realizations of its statistically determined parameters to compute ensemble-average values for the fitted parameters. To manage this computational burden, we implemented the fitting procedure on multiple processors of the Vermont Advanced Computing Center.

## RESULTS

### Progression of VILI in Mice

An example of the measurements of  $H$  made during a sequence of derecruitability tests in a single mouse is shown in Fig. 1. These observations show that lung derecruitability, as assessed by the rises in  $H$  observed during each 4.5 min test, increased progressively and dramatically over the 4 h ventilation period, indicating accelerating development of VILI throughout the experiment. In order to quantify the changes in derecruitability, we fit each set of rising  $H$  values with a straight line segment as illustrated in Fig. 1. The slope of each line segment was taken as the derecruitment rate ( $D_{\text{Rate}} = dH/dt$ ). The value of each line segment 20 s after the cessation of high  $V_t$  ventilation, termed  $H_1$ , represents the first recorded measurement of  $H$ . The time course of VILI development is thus characterized by the temporal increases in  $H_1$  and  $D_{\text{Rate}}$ .

We found that the acceleration of  $H_1$  over time increased with increasing  $V_t$ , so we were able to use  $V_t$  to titrate the rate of VILI development in the mice. For the four different  $V_t$  used in our experiments we found the time course of  $H_1$  to be well described by the empirical equation

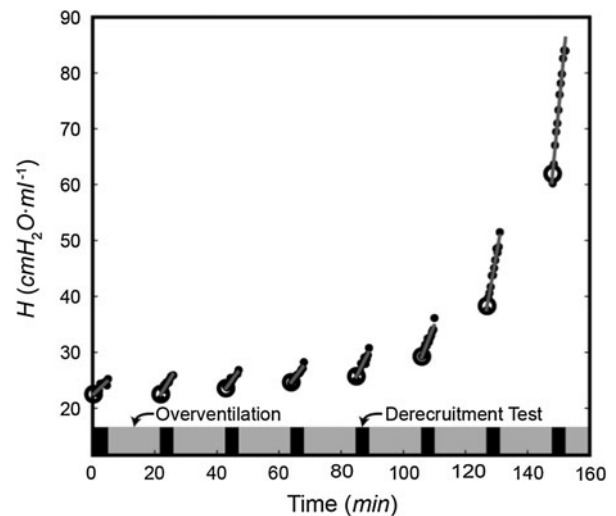


**FIGURE 1.** Elastance (filled circles) measured during each derecruitability test in a representative mouse (the durations of the derecruitability tests are indicated by the black regions in the horizontal bar along the time axis). During the overventilation periods (indicated by the gray regions in the horizontal bar) the mouse received  $V_t = 1.2 \text{ mL}$ . Also shown are the straight-line fits (lines) to  $H$  during each derecruitment test. The slopes of the fitted lines define the derecruitment rate,  $D_{\text{Rate}}$ , during each test. The values of the fitted lines corresponding to the first measurement of  $H$  in each test, defined as  $H_1$ , are indicated by large open circles.

$$H_1(t) = \tau_H t^4 + H_1^0, \quad (5)$$

where  $H_1^0$  corresponds to  $H_1$  in a healthy lung, and  $\tau_H$  represents the rate of VILI development. The mean ( $\pm$  SD) values of  $H_1$  and the fits provided by Eq. (5) are shown in Fig. 2 for the four groups of mice, while their respective mean best-fit values of  $\tau_H$  and  $H_1^0$  are given in Table 1. We also found that the values of  $D_{Rate}$  and  $H_1$  obtained from the four groups all lay along a single relationship as shown in Fig. 3. This relationship was well described by the empirical equation

$$D_{Rate} = 5.28 \ln(H_1) - 16.13 \quad (6)$$

Given that both  $D_{Rate}$  and  $H_1$  provide sensitive reflections of the degree of VILI in initially normal mice, as illustrated in Fig. 1, it follows that the degree of VILI can be uniquely specified in terms of either of  $D_{Rate}$  or  $H_1$ .

Figure 4 shows the peak tracheal pressure ( $\widehat{P}_{Tr}$ ) from the four different  $V_t$  groups. In contrast to both  $D_{Rate}$  and  $H_1$ ,  $\widehat{P}_{Tr}$  increased linearly in all groups at a rate that was independent of  $V_t$ . The parameter values for the lines fit to  $\widehat{P}_{Tr}$  vs. time are given in Table 2.

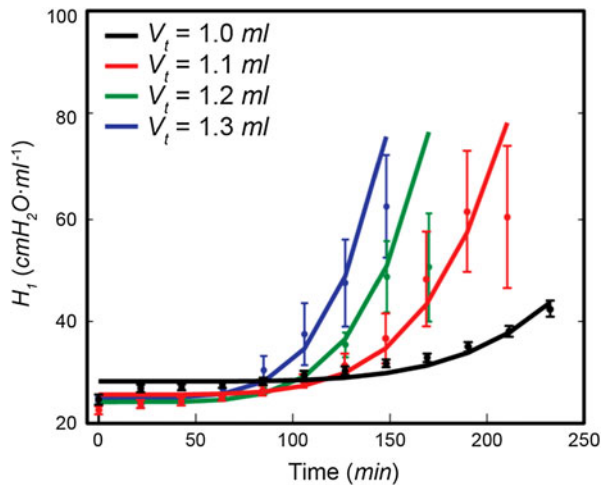


FIGURE 2. Mean ( $\pm$  SD) values of  $H_1$  for each derecruitability test in each of the four groups of mice together with the fits provided by Eq. (5) to each group (solid lines).

TABLE 1. Parameter values obtained by fitting Eq. (5) to the  $H_1$  data from the four groups of mice.

$V_t$ (mL)	Number of animals	$H_1^0$ (cmH <sub>2</sub> O)	$\tau_H$ ( $\pm$ SD) (cmH <sub>2</sub> O t <sup>-4</sup> )	$R^2$
1.0	6	26.8	$5.3 (\pm 1.2) \times 10^{-9}$	0.94
1.1	6	23.6	$2.5 (\pm 1.2) \times 10^{-8}$	0.94
1.2	5	22.5	$5.4 (\pm 2.3) \times 10^{-8}$	0.98
1.3	6	23.5	$9.6 (\pm 5.9) \times 10^{-8}$	0.96

### Computational Modeling of VILI Progression

In attempting to use the computational model described in Materials and Methods to mimic the above experimental data, we had to choose distributions from which to randomly draw values for  $P_o$ ,  $P_c$ ,  $s_o$  and  $s_c$ , as this is what determines the dynamics of recruitment and derecruitment predicted by the model. Experimental data upon which to base these distributions, however, are scant. In two previous studies<sup>7,22</sup> we assumed that  $P_o$  and  $P_c$  are distributed in a Gaussian fashion based on reports in patients.<sup>9,29</sup> We also assumed that  $s_c$  and  $s_o$  would come from monotonically decreasing probability distributions because there is no apparent limit to how rapidly a lung unit might open or close. We therefore

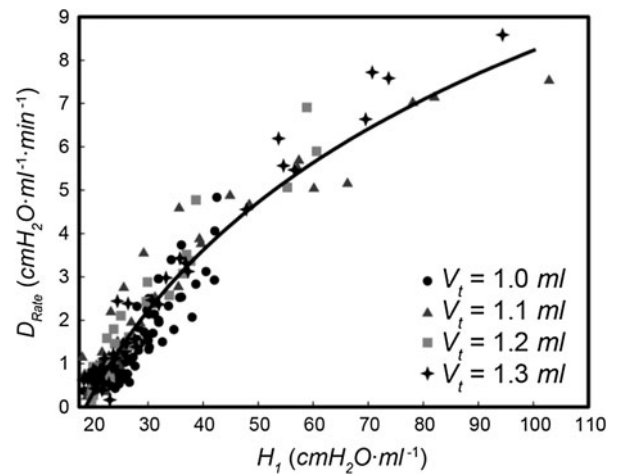


FIGURE 3. Relationship between  $H_1$  and  $D_{Rate}$  for all animals together with the fit provided by Eq. (6) ( $R^2 = 0.91$ ).

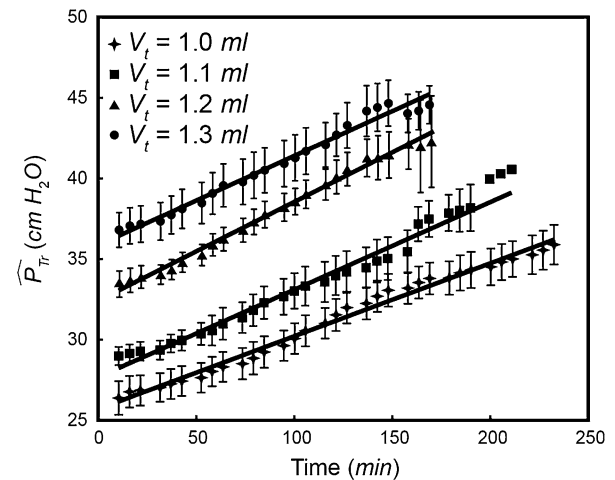


FIGURE 4. Peak tracheal pressure (mean  $\pm$  SD) measured at 5.5 min intervals during over-ventilation (symbols), together with linear fits (solid lines).

arbitrarily assumed exponential distributions for  $s_c$  and  $s_o$ . Accordingly,  $P_c$  was drawn from a Gaussian distribution with a mean  $\mu_a = 0$  and standard deviation  $\sigma_a = 3$ , as suggested by Massa *et al.*,<sup>22</sup> and  $P_o = P_c + \Delta P$  where  $\Delta P = 4$  cmH<sub>2</sub>O.  $s_o$  and  $s_c$  were drawn from exponential distributions (probability density function  $f(x) = \lambda e^{-\lambda x}$ ) with rate constants  $\lambda_c^a = 1000$  and  $\lambda_o^a = 50$ , respectively, so that airway closure occurred an order of magnitude faster than airway opening, as we found previously.<sup>22</sup>

We found that the computational model described above gave the best recapitulations of the experimen-

tally observed  $H_1$  and  $D_{Rate}$  (Fig. 5) if we let  $\mu_a$  increase linearly with time after a  $V_t$ -dependent critical time  $t_{crit}$  was reached. That is,

$$\mu_a = \begin{cases} 0 & t < t_{crit} \\ \alpha_1(t - t_{crit}) & t \geq t_{crit} \end{cases} \quad (7)$$

where  $\alpha_1$  is a constant (the fitted values of  $\alpha_1$  and  $t_{crit}$  for the four groups are given in Table 3).

In order to mimic the observed accelerating increase in  $H_1$  while maintaining a linear increase in pressure, we found it necessary to invoke a second population of airways that open and close very rapidly at high pressures and that increase in number as VILI progresses. For this subgroup of airways,  $P_c$  is selected from a normal distribution with a mean  $\mu_b = 18.0$  and standard deviation  $\sigma_b = 3.0$ , while  $\Delta P = 0.1$ ,  $\lambda_c^b = 0.03$  and  $\lambda_o^b = 1 \times 10^{-3}$ . The number of airways exhibiting this behavior ( $N_{HP}$ ) increases with time according to the degree of lung injury as

$$N_{HP} = \begin{cases} 0 & t < t_{crit} \\ \alpha_2(t - t_{crit})^{1.25} & t \geq t_{crit} \end{cases} \quad (8)$$

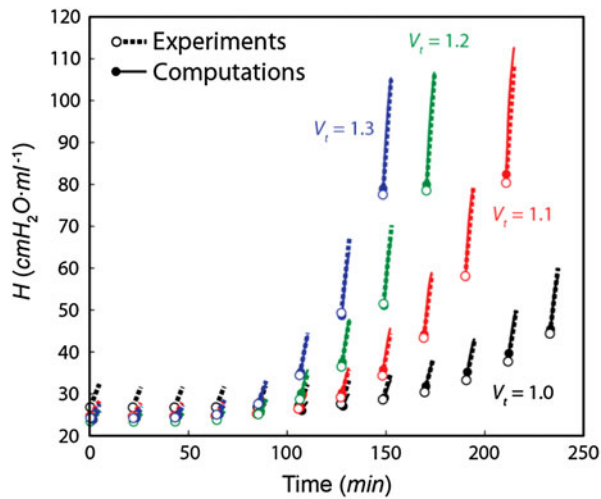
The fitted values of  $\alpha_2$  are given in Table 3. By using two groups of respiratory units, together with Eq. (1), this model is capable of reproducing the VILI-induced alterations in elastance (Fig. 5) and peak pressure (Fig. 6) observed experimentally.

Figure 7 shows the model predictions of the fraction of airways that are open as a function of time over the course of the entire experiment for  $V_t = 1.2$  mL. The dashed lines in the figure show the amount of rapid derecruitment that occurs at the beginning of each derecruitability test. This highlights the acceleration in the number of rapidly closing airways as VILI progresses.

Finally, we evaluated the sensitivity of the model to variations in its key parameters by comparing the best-fit predictions for  $V_t = 1.2$  mL, shown in Fig. 5, to the predictions made by altering each of the parameters in question by  $\pm 5\%$ . We quantified sensitivity in terms of the maximum root mean square errors (RMSE) in  $\widehat{P}_{tr}$  and  $H$  (Fig. 8), determined at time-points identical to the experiments. The sensitivity of the model to  $\mu_a$ , which is initially 0, is evaluated at  $\mu_a = \pm 0.377$ , a value which corresponds to  $\pm 5\%$  changes in the cumulative distribution function. Note that a degree of variation is inherent due to the statistical nature of the model, despite each model run consisting of the average of 256 independent simulations. This baseline level of variation is computed by comparing two runs without changing the parameters, and is labeled “No Change” in Fig. 8.

**TABLE 2. Parameters values of straight line fits to  $\widehat{P}_{tr}$  vs. time for the four groups of mice.**

$V_t$ (mL)	Slope (cmH <sub>2</sub> O min <sup>-1</sup> )	Intercept (cmH <sub>2</sub> O)	$R^2$
1.0	0.045	25.7	0.64
1.1	0.052	28.0	0.83
1.2	0.061	32.4	0.69
1.3	0.055	35.9	0.45



**FIGURE 5. Elastance during each derecruitability test in the four groups of mice as shown in Fig. 5 (dashed lines) together with the values produced by the computational model (solid lines).**

**TABLE 3. Parameter values obtained by fitting Eqs. (7) and (8) to the data from the four groups of mice.**

$V_t$ (mL)	$\alpha_1$ (cmH <sub>2</sub> O min <sup>-1</sup> )	$\alpha_2$ (min <sup>-1.25</sup> )	$t_{crit}$ (min <sup>-1.25</sup> )
1.0	0.025	$8.00 \times 10^{-4}$	115
1.1	0.05	$1.58 \times 10^{-3}$	98
1.2	0.05	$2.18 \times 10^{-3}$	82
1.3	0.05	$2.56 \times 10^{-3}$	70

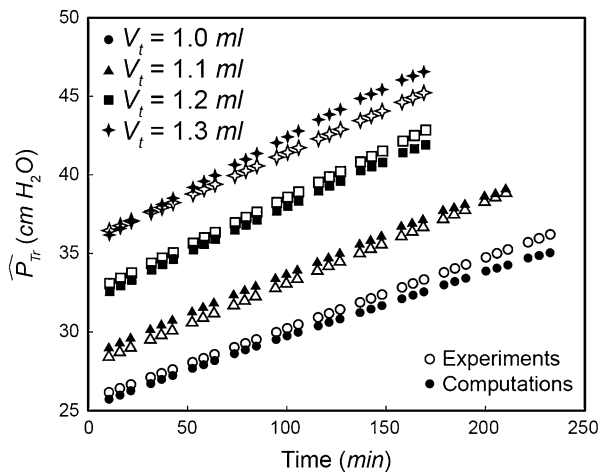


**FIGURE 6.** Peak pressures during over-ventilation measured in the four groups of mice (open symbols) together with the values produced by the computational model (closed symbols).

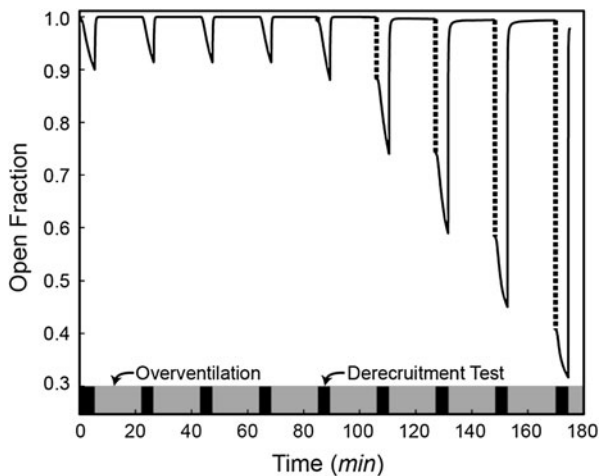


**FIGURE 7.** Predicted fraction of open lung units in the computational model with  $V_t = 1.2$  mL as a function of time throughout the 4 h period of mechanical ventilation. Note the rapid derecruitment occurring at the beginning of each derecruitment test (dashed lines).

## DISCUSSION

ALI is a relatively common form of acute non-cardiogenic pulmonary edema that can result from a variety of insults, including massive hemorrhage, systemic infection, and inhalation of noxious agents. The severe form of ALI known as ARDS has a mortality of 30–40% and is frequently treated with mechanical ventilation, which may lead to VILI. Despite the prevalence and high mortality of VILI, the mechanics of injury and the resulting effects on lung function are not fully characterized. This is due in part to the myriad of factors, ranging from the host immune response to surfactant inactivation, which interact to produce VILI. In the current study we have built on an

earlier investigation<sup>34</sup> to produce a mouse model of VILI in which the rate of lung injury development can be titrated through choice of the  $V_t$  used to over-ventilate the lungs against a PEEP of zero (Figs. 2, 4). The  $V_t$  we used to achieve VILI are, of course, significantly larger than those that would normally be applied in even a perfectly healthy mouse. Our goal here, however, is to understand how VILI develops in the normal lung over an experimental tractable timescale, and for that we must push the organ to its mechanical limits.

We characterize the physiological effects of VILI by monitoring how lung elastance increases over the first few minutes immediately following a recruitment maneuver since injury of the lung accelerates the rate and magnitude of this increase. Also, we have shown previously, using both *in vivo* microscopy<sup>2</sup> and computed tomography,<sup>5</sup> that these increases in elastance reflect commensurate increases in the amount of derecruited lung. Accordingly, we take the transient increases in elastance following a recruitment maneuver to constitute a measure of what we call the derecruitability of the lung. In this study we found that derecruitability can be characterized to a large extent by only two parameters, as illustrated in Fig. 1. One of these parameters is the first measurement of elastance ( $H_1$ ) made 20 s following the cessation of large  $V_t$ . As the preceding large  $V_t$  serve to recruit most of the lung,  $H_1$  reflects the extent to which the lung has been able to derecruit during this brief period of time. The second parameter ( $D_{\text{Rate}}$ ) reflects the rate of increase of elastance over the subsequent 4 min.  $H_1$  thus describes how derecruitment takes place on a timescale of seconds, while  $D_{\text{Rate}}$  characterizes derecruitment dynamics over a timescale of minutes. Together,  $H_1$  and  $D_{\text{Rate}}$  provide a precise link between lung function and injury status.

Intriguingly,  $H_1$  and  $D_{\text{Rate}}$  appear to be tightly linked to each other, as shown in Fig. 3. In other words, either  $H_1$  or  $D_{\text{Rate}}$  on its own is sufficient to uniquely specify a given degree of VILI, at least as it develops in initially normal mice. This means we can use the relationship embodied in Fig. 3 and Eq. (6) to reproduce a complete set of derecruitability measurements from a set only of  $H_1$  values. This is done in Fig. 5 (dashed lines) by using Eqs. (5) and (6) and the parameter values in Table 1 to recapitulate the complete set of derecruitability measurements for all  $V_t$  groups. The rate of acceleration of VILI in initially normal mice can thus be titrated through control of the magnitude of the over-ventilation  $V_t$ . It remains to be seen whether the relationship shown in Fig. 3, and quantified in Eq. (6), is truly universal (i.e., applies to mice with ALI caused by other factors), but we can conclude from the present study that over-ventilation

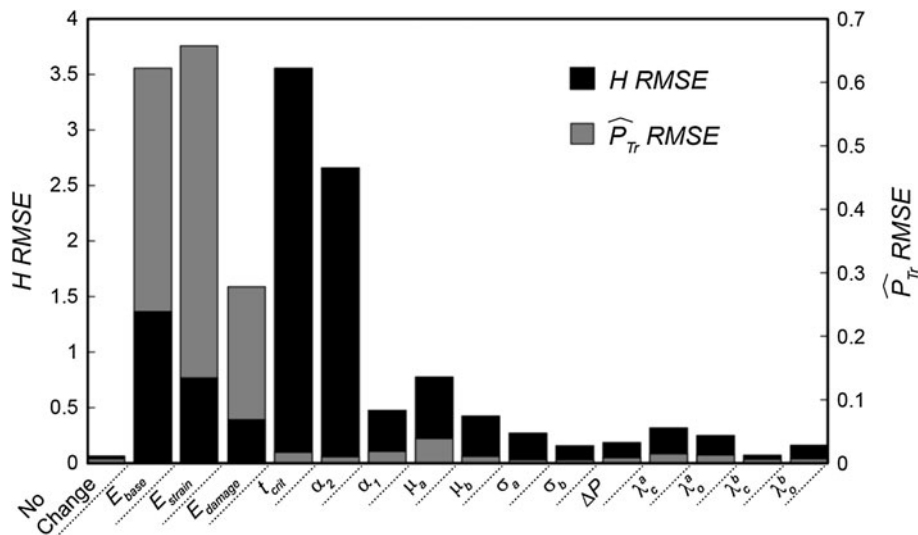


**FIGURE 8.** Sensitivity analysis showing the maximum change in RMSE for  $H$  (black) and  $\widehat{P}_{Tr}$  (gray) with a  $\pm 5\%$  change in the listed variables at  $V_t = 1.2$  mL.

of normal mice sets the lungs on a unique path to destruction. Varying  $V_t$  simply varies the rate of travel down this path.

We speculated in a previous study<sup>34</sup> that the accelerating increase in derecruitability seen with over-ventilation at zero PEEP reflects a positive feedback mechanism whereby injury begins with a small leakage of fluid and/or protein into the airspaces, which disrupts surfactant function.<sup>10,18,19,35</sup> This then increases the stresses of mechanical ventilation, making the leak worse, raising surface tension even further, and so on. The universality of the  $H_1$ – $D_{Rate}$  relationship found in the present study (Fig. 3) supports this hypothesis by suggesting that increasing  $V_t$  simply increases the rate at which material leaks into the airspaces. Also, because of the link between  $H_1$  and  $D_{Rate}$  shown in Fig. 3, the rate of development of VILI for a particular  $V_t$  can be encapsulated in a single parameter characterizing the rate of acceleration of  $H_1$  with time. This parameter is  $\tau_H$  in Eq. (5), and is strongly dependent on  $V_t$  (Table 1; Fig. 2), further demonstrating that we are able to use  $V_t$  to titrate our mouse model of VILI to obtain different rates of injury development.

Figure 2 and Table 1 show that  $H_1^0$ , obtained from the  $H_1$  fit, is higher for the  $V_t = 1.0$  mL group compared to the other groups. This difference in  $H_1^0$  arises not from the difference in the first derecruitability test, but in differences observed in the second (and subsequent) tests. A two-way analysis of variance comparing  $H_1$  for the four  $V_t$  groups during the first and second derecruitability tests shows a significant difference ( $p = 0.05$ ) between the  $V_t = 1.0$  mL and the higher- $V_t$  groups during the second derecruitability test. There is no significant difference during the first

test. Because all values of  $H_1$  are given equal weight in the  $H_1$  fit (Eq. (5)), the fit values of  $H_1^0$  (Table 1) are higher at  $V_t = 1.0$  mL. We hypothesize that this difference arises because a fraction of the lung is derecruited during the first over-ventilation epoch when  $V_t = 1.0$  mL, but this fraction becomes recruited with the higher  $V_t$ .

We showed in our previous study<sup>34</sup> that accelerating derecruitability of the kind seen in Figs. 2 and 5 can be qualitatively reproduced computationally by imposing an increase in the mean values of the distributions from which  $P_o$  and  $P_c$  are drawn. This makes biophysical sense because increases in airway opening and closing pressures are thought, on the basis of *in vitro* studies,<sup>8,15,25,30,31</sup> to reflect an increase in surface tension at the air–liquid interface in the lungs, something that is known to occur in ARDS. This motivated us to attempt to mimic the data in the present study in the same way. Here, however, we varied the rates of increase of the distribution means for  $P_o$  and  $P_c$  (i.e.,  $\mu_a$ ) in order to account for the four  $V_t$ -dependent rates of VILI we observed experimentally in the mice (that is, we varied the value of  $\alpha_1$  in Eq. (7)). This yielded qualitative agreement with the increases in  $D_{Rate}$  observed during the derecruitment tests, but it failed to mimic the concomitant increases in  $H_1$  (model results not shown). Noting that  $H_1$  reflects rapid derecruitment events that take place within the first 20 s following cessation of high  $V_t$  ventilation, we were led to include another distinct population of rapidly closing units in the model. This allowed the model to accurately mimic all the key features of our experimental data (Figs. 5, 6). The second population of units

increased in number as injury progressed (Eq. (8) and Table 3), and might correspond, for example, to those described in rats with VILI by Pavone *et al.*<sup>27</sup> These investigators used *in vivo* video microscopy to observe a population of damaged alveoli that recruit and derecruit extremely rapidly over the course of a single breath. Such alveolar instability is known to increase as VILI progresses and is attributed to surfactant inactivation.<sup>28</sup>

We also had to deal with the somewhat surprising observation that  $\widehat{P}_{tr}$  increased linearly at a rate that, contrary to both  $H_1$  and  $D_{Rate}$ , did not depend on  $V_t$  as shown in Fig. 4. (Note that the vertical differences in the  $\widehat{P}_{tr}$  relationships between the different  $V_t$  groups in Fig. 4 are simply a consequence of the nonlinear pressure–volume relationship of the lung.) A possible explanation for the behavior of  $\widehat{P}_{tr}$  is that an increase in surface tension causes an increase in the intrinsic stiffness of those respiratory units that are open at any given point in time. However, the  $V_t$ -independence of the linear increases in  $\widehat{P}_{tr}$  suggests a mechanism that is distinct from that causing the  $V_t$ -dependent increases in derecruitability. One possibility is that the increases  $\widehat{P}_{tr}$  reflect alveolar flooding due to the accumulation of fluid in the distal airspaces.

Our current working hypothesis about the link between lung function and VILI thus involves the following three distinct components: (1) progressive decrements in surfactant function cause a small but increasing population of unstable alveoli to close almost immediately<sup>27</sup> following the transition from high to low  $V_t$  at the start of each derecruitability test, giving rise to the accelerating increases in  $H_1$  as VILI develops, (2) increasing surface tension also causes an increasing number of small airways to close at a slower rate during the derecruitability tests *via* liquid bridging,<sup>22</sup> giving rise to the accelerating increases in  $D_{Rate}$ , and (3) epithelial leak results in accumulation of fluid in the airspaces which results in increased overdistention at a prescribed lung volume, giving rise to the linear increases in  $\widehat{P}_{tr}$ .

A corollary of the above interpretation is the implication that while a deep inspiration will rapidly recruit the severely injured lung, as shown in Fig. 7, much of this improvement is short lived because when pressure returns to a normal level a significant fraction of the lung will derecruit again almost immediately (Fig. 7, dashed lines). As a consequence, there will be a great deal of repeated closure and reopening of large regions of the injured lung that will likely exacerbate atelectrauma. At the same time, the remaining open regions will become over-distended during each inspiration, possibly leading to enhanced volutrauma in these regions. The computational model we have

developed here may thus be useful for exploring the relative benefits of ventilator modes that vary in their degrees of mean lung pressure and pressure excursion, such as airway pressure-release ventilation and high-frequency ventilation.

The relative importance of the various physiological mechanisms represented in our model on the progression of VILI is indicated by the results of the sensitivity analysis shown in Fig. 8. Interestingly, the variations in model parameter values have different consequences for  $H$  and  $\widehat{P}_{tr}$ . Specifically,  $H$  is most strongly influenced by  $t_{crit}$  and  $\alpha_2$  which determine, *via* Eq. (8), the kinetics of the subgroup of airways that appear as injury progresses, yet both parameters have minimal effect on  $\widehat{P}_{tr}$ . Conversely, the parameters that determine tissue elastance properties *via* Eq. (1), particularly the volume dependence of elastance ( $E_{strain}$ ), play the dominant role in determining  $\widehat{P}_{tr}$ . These results support the notion that the temporal changes in  $H$  and  $\widehat{P}_{tr}$  reflect complementary, yet different, aspects of the tissue injury that is caused by mechanical ventilation.

Finally, although we have argued above that certain biophysical events in the lung are responsible for the observed derangements in mechanical function seen in mice as VILI develops, much of this has been achieved with the aid of a computational model that is itself based on numerous assumptions, some of which are rather arbitrary. Accordingly, we must acknowledge that the limitations of the model translate directly into limitations of the study as a whole. The model is necessarily simple in terms of its structure because we wished to minimize the number of free parameters that had to be adjusted when fitting it to the experimental data. Consequently, although the model recapitulated the main features of the experimental data, it did not have enough degrees of freedom to describe all the deterministic variation in the data, as evidenced by the modest but consistent over- and under-predictions of the data seen in Figs. 5 and 6. We therefore take the fitted model parameter values as general estimates of the magnitudes of the physiological quantities they represent, rather than precise estimates, which is appropriate in view of the fact that the model structure is also only an approximation to reality. For example, we represented the distributed nature of the lung in terms of a large number of parallel airways having equal diameter and resistance, which does not mimic the branching structure of the airway tree. Although we have previously extended our model to include a branching tree containing airways of variable diameter,<sup>21</sup> airway recruitment and derecruitment in the injured lung likely occurs mostly in the lung periphery. We therefore felt that representing this phenomenon



in terms of identical small parallel airways is reasonable. This, however, raises the possibility of mechanical interdependence between adjacent airways, mediated by the intervening parenchyma, which could have an important influence on how recruitment and derecruitment of a given airways affects, for example, the critical opening and closing pressures of its neighbors. This could result in spatial correlation between the behaviors of different lung units. These and other physiological details may need to be included in future versions of the model in order to improve the accuracy of its predictions, once the necessary data become available.

Another important assumption in the model is the heuristic scheme based on virtual trajectories that we employed to account for the dynamics of recruitment and derecruitment. The virtual trajectory variable  $x$  does not correspond to anything physical in particular, even though the behavior of  $x$  is reminiscent of the way in which liquid bridge formation and breakage have been shown to occur in table-top models *in vitro*<sup>8,14,36–38</sup> and in computational models.<sup>11–13,17,20</sup> Consequently, our choices for distributions of the open and closing pressures and velocities for the individual units in the model are purely empirical. Furthermore, we have not exhaustively demonstrated that the distributions we used in the model to account for our experimental findings are the only ones that would work. Rather, we have established the plausibility of various hypotheses, setting the scene for future experimental tests.

In summary, we have demonstrated in a mouse model of VILI that lung derecruitability increases in an accelerating manner that depends on  $V_t$ , while  $\widehat{P}_{tr}$  increases linearly in a manner that is independent of  $V_t$ . Derecruitment, which reflects injury severity, is observed on timescales ranging from seconds to minutes as quantified by the parameters  $H_1$  and  $D_{Rate}$ , respectively.  $H_1$  and  $D_{Rate}$  are linked through a single relationship, which suggests they may share a common mechanistic basis. By contrast,  $\widehat{P}_{tr}$  increases at a linear rate that is independent of  $V_t$ . Experimentation with a computational model suggests that the increases in  $H_1$  and  $D_{Rate}$  may be due to progressive increases in surface tension at the air–liquid interface in the lung as surfactant function becomes compromised by fluid and plasma proteins leaking into the airspaces, with  $H_1$  reflecting rapid closure of alveoli and  $D_{Rate}$  reflecting slower closure of small airways.  $\widehat{P}_{tr}$ , on the other hand, appears to be affected through a different biophysical mechanism, one possibility being the irreversible flooding of alveoli with fluid that has leaked into the airspaces. The computational model also predicts that recruitment and derecruitment of substantial fractions of the lung occur over a wide range of times scales in severe VILI.

## ACKNOWLEDGMENTS

This work was supported by NIH grants P30 GM103532 and T32 HL076122. Computational resources were provided by the Vermont Advanced Computing Core which is supported by NASA NNX-08AO96G.

## REFERENCES

- <sup>1</sup>The Acute Respiratory Distress Syndrome Network. Ventilation with lower tidal volumes as compared with traditional tidal volumes for acute lung injury and the acute respiratory distress syndrome. *N. Engl. J. Med.* 342:1301–1308, 2000.
- <sup>2</sup>Albert, S. P., J. DiRocco, G. B. Allen, J. H. T. Bates, R. Lafollette, B. D. Kubiak, J. Fischer, S. Maroney, and G. F. Nieman. The role of time and pressure on alveolar recruitment. *J. Appl. Physiol.* 106:757–765, 2009.
- <sup>3</sup>Allen, G., and J. H. Bates. Dynamic mechanical consequences of deep inflation in mice depend on type and degree of lung injury. *J. Appl. Physiol.* 96:293–300, 2004.
- <sup>4</sup>Allen, G., L. K. Lundblad, P. Parsons, and J. H. Bates. Transient mechanical benefits of a deep inflation in the injured mouse lung. *J. Appl. Physiol.* 93:1709–1715, 2002.
- <sup>5</sup>Allen, G. B., T. Leclair, M. Cloutier, J. Thompson-Figueroa, and J. H. Bates. The response to recruitment worsens with progression of lung injury and fibrin accumulation in a mouse model of acid aspiration. *Am. J. Physiol. Lung Cell. Mol. Physiol.* 292:L1580–L1589, 2007.
- <sup>6</sup>Bates, J. H. T. Lung Mechanics. An Inverse Modeling Approach. Cambridge: Cambridge University Press, 2009.
- <sup>7</sup>Bates, J. H. T., and C. G. Irvin. Time dependence of recruitment and derecruitment in the lung: a theoretical model. *J. Appl. Physiol.* 93:705–713, 2002.
- <sup>8</sup>Cassidy, K. J., D. Halpern, B. G. Ressler, and J. B. Grotberg. Surfactant effects in model airway closure experiments. *J. Appl. Physiol.* 87:415–427, 1999.
- <sup>9</sup>Crotti, S., D. Mascheroni, P. Caironi, P. Pelosi, G. Ronzoni, M. Mondino, J. J. Marini, and L. Gattinoni. Recruitment and derecruitment during acute respiratory failure: a clinical study. *Am. J. Respir. Crit. Care Med.* 164:131–140, 2001.
- <sup>10</sup>Fuchimukai, T., T. Fujiwara, A. Takahashi, and G. Enhorning. Artificial pulmonary surfactant inhibited by proteins. *J. Appl. Physiol.* 62:429–437, 1987.
- <sup>11</sup>Fujioka, H., and J. B. Grotberg. Steady propagation of a liquid plug in a 2D-channel. *J. Biomech. Eng.* 126:567–577, 2004.
- <sup>12</sup>Fujioka, H., and J. B. Grotberg. Steady propagation of a surfactant laden liquid plug in a 2D-channel. *Phys. Fluids* 17:Art. No. 082102, 2005.
- <sup>13</sup>Gaver, III, D. P., D. Halpern, O. E. Jensen, and J. B. Grotberg. The steady motion of a semi-infinite bubble through a flexible-walled channel. *J. Fluid Mech.* 319: 25–65, 1996.
- <sup>14</sup>Gaver, III, D. P., R. W. Samsel, and J. Solway. Effects of surface tension and viscosity on airway reopening. *J. Appl. Physiol.* 69:74–85, 1990.
- <sup>15</sup>Halpern, D., and J. B. Grotberg. Surfactant effects on fluid-elastic instabilities of liquid-lined flexible tubes. *J. Fluid Mech.* 244:615–632, 1993.

- <sup>16</sup>Hantos, Z., B. Daroczy, B. Suki, S. Nagy, and J. J. Fredberg. Input impedance and peripheral inhomogeneity of dog lungs. *J. Appl. Physiol.* 72:168–178, 1992.
- <sup>17</sup>Heil, M. Airway closure: occluding liquid bridges in strongly buckled elastic tubes. *J. Biomech. Eng.* 121:487–493, 1999.
- <sup>18</sup>Holm, B. A., and R. H. Notter. Effects of hemoglobin and cell-membrane lipids on pulmonary surfactant activity. *J. Appl. Physiol.* 63:1434–1442, 1987.
- <sup>19</sup>Holm, B. A., R. H. Notter, and J. N. Finkelstein. Surface property changes from interactions of albumin with natural lung surfactant and extracted lung lipids. *Chem. Phys. Lipids* 38:287–298, 1985.
- <sup>20</sup>Howell, P. D., S. L. Waters, and J. B. Grotberg. The propagation of a liquid bolus along a liquid-lined flexible tube. *J. Fluid Mech.* 406:309–335, 2000.
- <sup>21</sup>Ma, B., and J. H. T. Bates. Modeling the complex dynamics of derecruitment in the lung. *Ann. Biomed. Eng.* 38:3466–3477, 2010.
- <sup>22</sup>Massa, C. B., G. B. Allen, and J. H. T. Bates. Modeling the dynamics of recruitment and derecruitment in mice with acute lung injury. *J. Appl. Physiol.* 105:1813–1821, 2008.
- <sup>23</sup>Matthay, M. A., S. Bhattacharya, D. Gaver, L. B. Ware, L. H. Lim, O. Syrkina, F. Eyal, and R. Hubmayr. Ventilator-induced lung injury: in vivo and in vitro mechanisms. *Am. J. Physiol. Lung Cell. Mol. Physiol.* 283:L678–L682, 2002.
- <sup>24</sup>Matthay, M. A., L. B. Ware, and G. A. Zimmerman. The acute respiratory distress syndrome. *J. Clin. Investig.* 122:2731–2740, 2012.
- <sup>25</sup>Naureckas, E. T., C. A. Dawson, B. S. Gerber, D. P. Gaver, III, H. L. Gerber, J. H. Linehan, J. Solway, and R. W. Samsel. Airway reopening pressure in isolated rat lungs. *J. Appl. Physiol.* 75:1323–1333, 1994.
- <sup>26</sup>Nelder, J. A., and R. Mead. A simplex method for function minimization. *Comput. J.* 7:308–313, 1965.
- <sup>27</sup>Pavone, L., S. Albert, J. DiRocco, L. Gatto, and G. Nieman. Alveolar instability caused by mechanical ventilation initially damages the nondependent normal lung. *Crit. Care* 11:R104, 2007.
- <sup>28</sup>Pavone, L. A., S. Albert, D. Carney, L. A. Gatto, J. M. Halter, and G. F. Nieman. Injurious mechanical ventilation in the normal lung causes a progressive pathologic change in dynamic alveolar mechanics. *Crit. Care* 11:1–9, 2007.
- <sup>29</sup>Pelosi, P., M. Goldner, A. McKibben, A. Adams, G. Eccher, P. Caironi, S. Losappio, L. Gattinoni, and J. J. Marini. Recruitment and derecruitment during acute respiratory failure: an experimental study. *Am. J. Respir. Crit. Care* 164:122–130, 2001.
- <sup>30</sup>Perun, M. L., and D. P. Gaver III. An experimental model investigation of the opening of a collapsed untethered pulmonary airway. *J. Biomech. Eng.* 117:245–253, 1995.
- <sup>31</sup>Perun, M. L., and D. P. Gaver III. The interaction between airway lining fluid forces and parenchymal tethering during pulmonary airway reopening. *J. Appl. Physiol.* 75:1717–1728, 1995.
- <sup>32</sup>Salazar, E., and J. H. Knowles. An analysis of pressure-volume characteristics of the lungs. *J. Appl. Physiol.* 19:97–104, 1964.
- <sup>33</sup>Schuessler, T. F., and J. H. Bates. A computer-controlled research ventilator for small animals: design and evaluation. *IEEE Trans. Biomed. Eng.* 42:860–866, 1995.
- <sup>34</sup>Seah, A. S., K. A. Grant, M. Aliyeva, G. B. Allen, and J. H. T. Bates. Quantifying the roles of tidal volume and PEEP in the pathogenesis of ventilator-induced lung injury. *Ann. Biomed. Eng.* 39:1505–1516, 2011.
- <sup>35</sup>Seeger, W., G. Stohr, H. R. D. Wolf, and H. Neuhofer. Alteration of surfactant function due to protein leakage—special interaction with fibrin monomer. *J. Appl. Physiol.* 58:326–338, 1985.
- <sup>36</sup>Smith, B. J., E. Yamaguchi, and D. P. Gaver III. A translating stage system for  $\mu$ -PIV measurements surrounding the tip of a migrating semi-infinite bubble. *Meas. Sci. Technol.* 21:015401, 2010.
- <sup>37</sup>Zheng, Y., J. C. Anderson, V. Suresh, and J. B. Grotberg. Effect of gravity on liquid plug transport through an airway bifurcation model. *J. Biomech. Eng. Trans. ASME* 127:798–806, 2005.
- <sup>38</sup>Zheng, Y., H. Fujioka, J. C. Grotberg, and J. B. Grotberg. Effects of inertia and gravity on liquid plug splitting at a bifurcation. *J. Biomech. Eng.* 128:707–716, 2006.